



Structural hysteresis and hierarchy in adsorbed glycoproteins

Robert Horvath, James McColl, Gleb E. Yakubov, and Jeremy J. Ramsden

Citation: *The Journal of Chemical Physics* **129**, 071102 (2008); doi: 10.1063/1.2968127

View online: <http://dx.doi.org/10.1063/1.2968127>

View Table of Contents: <http://scitation.aip.org/content/aip/journal/jcp/129/7?ver=pdfcov>

Published by the [AIP Publishing](http://www.aip.org)

Articles you may be interested in

[Lipid-assisted protein transport: A diffusion-reaction model supported by kinetic experiments and molecular dynamics simulations](#)

J. Chem. Phys. **144**, 184901 (2016); 10.1063/1.4948323

[Natural zwitterionic organosulfurs as surface ligands for antifouling and responsive properties](#)

Biointerphases **9**, 029010 (2014); 10.1116/1.4869300

[Enhanced Wang Landau sampling of adsorbed protein conformations](#)

J. Chem. Phys. **136**, 114114 (2012); 10.1063/1.3691669

[Dynamic information for cardiotoxin protein desorption from a methyl-terminated self-assembled monolayer using steered molecular dynamics simulation](#)

J. Chem. Phys. **134**, 194705 (2011); 10.1063/1.3592559

[Understanding the nonfouling mechanism of surfaces through molecular simulations of sugar-based self-assembled monolayers](#)

J. Chem. Phys. **125**, 214704 (2006); 10.1063/1.2397681



NEW Special Topic Sections

NOW ONLINE
Lithium Niobate Properties and Applications:
Reviews of Emerging Trends

AIP Applied Physics Reviews

Structural hysteresis and hierarchy in adsorbed glycoproteins

Robert Horvath,¹ James McColl,^{1,a)} Gleb E. Yakubov,² and Jeremy J. Ramsden^{1,b)}

¹Department of Materials, Cranfield University, Bedfordshire MK43 0AL, United Kingdom

²Unilever Corporate Research, Colworth Park, Bedfordshire MK44 1LQ, United Kingdom

(Received 14 May 2008; accepted 16 July 2008; published online 21 August 2008)

The adsorption and desorption of the giant heavily glycosylated protein mucin from solutions of different bulk concentrations have been followed at the nanometer scale using high resolution molecular microscopy based on optical waveguide lightmode spectroscopy. Modeling the layer as a uniaxial thin film allowed the *in situ* determination of adsorbed mass, mean layer thickness, and structural anisotropy. These parameters manifest highly significant adsorption-desorption hysteresis, indicating at least two dominant glycoprotein conformational types (i.e., molecular states, structurally and kinetically distinguishable). One of them is proposed to be a conformationally extended state that engenders uniaxial symmetry and dominates layers generated from low bulk concentrations. The revealed structure and the mechanism by which it is formed are postulated to be a general feature of the self-assembly of large glycoproteins. We expect that, *inter alia*, this knowledge will be relevant for understanding the extraordinary effectiveness of mucin thin films as boundary lubricants. © 2008 American Institute of Physics. [DOI: 10.1063/1.2968127]

Proteins are complex macromolecules with definite structures and a small number of dominant degrees of freedom.¹ They typically exhibit two or more stable conformational states separated by moderate energy barriers, and therefore possess memory. In this respect they differ from more regular, or more random, synthetic organic polymers.² This attribute has been demonstrated in the context of the adsorption of proteins at solid/liquid interfaces both theoretically³ and experimentally.^{4–6} Compact globular proteins (such as the abundant soluble proteins of the blood, e.g., albumin and transferrin) have been extensively investigated for decades, and many features of their behavior are understood; highly elongated fibrous proteins are known to follow more complicated multistructural trajectories (e.g., Refs. 7 and 8), and not all details of their adsorption and desorption processes have as yet been elucidated; even less is presently known about an even more complex class of objects, giant glycoproteins such as mucin, which have only recently become available in sufficiently high purity to permit truly quantitative experimentation with them.

The mucin family of glycoproteins is ubiquitous within living organisms, especially as a surface coating, where it fulfils above all a role of lubricating surfaces rubbing against each other.^{9,10} Although, like all proteins, the mucins have a single unbranched polypeptide chain as a backbone, typically 50%–75% of their mass is constituted from oligosaccharides, attached as numerous short branches along the polypeptide backbone.

Optical waveguide lightmode spectroscopy^{11–13} (OWLS) has been extensively used to determine the kinetics of pro-

tein monolayer^{8,12} and multilayer¹⁴ self-assembly, but the resulting structures have typically been characterized solely by the number of assembled objects per unit area and the areas they occupy. Recent theoretical developments,¹⁵ not previously exploited for the analysis of experimental data, in analyzing the results from OWLS measurements now enable the kinetics of the development of optical anisotropy of the structures being self-assembled to be measured, greatly extending the power of OWLS for characterizing self-assembly processes. In particular, they allow the evolution of the molecular structure of thin films to be determined, since this is directly related to the optical anisotropy. Moreover, OWLS is a relatively simple and inexpensive technique and can be used *in situ* during assembly processes taking place at room temperature and pressure in aqueous media. Compared to techniques that have hitherto been applied, such as neutron diffraction,¹⁶ this greatly extends the scope of molecular probing of biological relevance.

Mucin is known to display liquid crystalline behavior,¹⁷ from which it follows that adsorbed thin films are very likely to be birefringent. Hence it seems to be essential to properly consider the anisotropy of self-assembled mucin thin films, unlike the “simple” protein layers that are merely and sufficiently characterized by the number of adsorbed molecules per unit area.

We have found that the evolution of the anisotropy of thin films that are first self-assembled, and then partly disassembled, shows a striking hysteresis, hitherto not reported for any protein self-assembly process.

Our starting material was a commercial preparation of porcine gastric mucin (“Orthana,” Denmark; molecular weight estimated as 545 kDa), which was extensively dialyzed against ultrapure water (Elga) and stored as a lyophilized powder before use. The polypeptide backbone of this mucin is decorated by relatively short branched oligosaccharide chains containing glucosamine and fructose residues (the

^{a)}Present address: University Chemical Laboratory, Lensfield Road, Cambridge, UK.

^{b)}Author to whom correspondence should be addressed. Tel.: +44 1234 754100. FAX: +44 1234 751346. Electronic mail: j.ramsden@cranfield.ac.uk.

“sparsely hyperbranched” structural category⁹) (overall, the saccharide constitutes somewhat more than 50% of the mass of the molecule, the rest being peptide).¹⁸ Solutions were freshly made up in ultrapure water. Adsorption substrata were thin (~ 170 nm) planar optical waveguides with a roughness of less than 1 nm made from $\text{Si}_x\text{Ti}_{1-x}\text{O}_2$, $x \approx 0.6$) incorporating a shallow (~ 5 nm) diffraction grating (2400 rulings/mm) (MicroVacuum, Budapest) for incoupling the light. Before use, the waveguides were cleaned in chromic acid, extensively rinsed in ultrapure water, then rinsed in a 2% aqueous solution of KOH, and again extensively rinsed in ultrapure water. Following that, they were placed in a hexamethyldisilazane (Sigma Aldrich) saturated environment at 74 °C for 5 h,¹⁹ resulting in a dense hydrophobic layer of short alkyl chains coating the waveguides.

A low-power linearly polarized helium-neon laser operating at wavelength $\lambda = 632.8$ nm was used to excite the TM_0 and TE_0 waveguide modes in the waveguide via incoupling at the diffraction grating; the incoupling angles measured being used to determine the propagation constants (effective refractive indices) of the guided lightmodes.

The waveguides were mounted so as to form one wall of a flow-through microcuvette through which the mucin solutions could be made to flow, and the whole assembly mounted on the ultraprecision goniometer of an OWLS-110 integrated optical scanner (MicroVacuum, Budapest) equipped with a TC-80 Peltier-based temperature controller, with which the incoupling angles were measured with micro-radian precision, from which the propagation constants (effective refractive indices) of the guided modes were calculated. All experiments were carried out at $T = 25.0$ °C.

The adsorbed mucin molecules can be approximated as a uniform thin film, since their thickness is much less than the wavelength of the probe light.²⁰ The film should not be assumed to be isotropic, but can be supposed to be birefringent and characterized optogeometrically by an average thickness d_A and ordinary and extraordinary refractive indices n_o and n_e . Since we only have two experimentally measured parameters (the effective refractive indices of the TM_0 and TE_0 lightmodes), we can only determine two unknown optogeometrical parameters, whereas three are required. To overcome this difficulty we constrained the average refractive index²¹ of the glycoprotein layer,

$$\langle n_A \rangle = \sqrt{(2n_o^2 + n_e^2)/3}, \quad (1)$$

to a value of 1.42.²² The four-layer mode equations, for mode numbers $m = 0, 1, 2, \dots$,^{15,23,24}

$$\begin{aligned} \pi m \approx & (2\pi/\lambda)(n_F^2 - N^2)^{1/2}(d_F + \Delta d_F) \\ & - \arctan \left[\left(\frac{n_F}{n_C} \right)^{2\rho} \left(\frac{N^2 - n_C^2}{n_F^2 - N^2} \right)^{1/2} \right] \\ & - \arctan \left[\left(\frac{n_F}{n_S} \right)^{2\rho} \left(\frac{N^2 - n_S^2}{n_F^2 - N^2} \right)^{1/2} \right], \quad (2) \end{aligned}$$

where

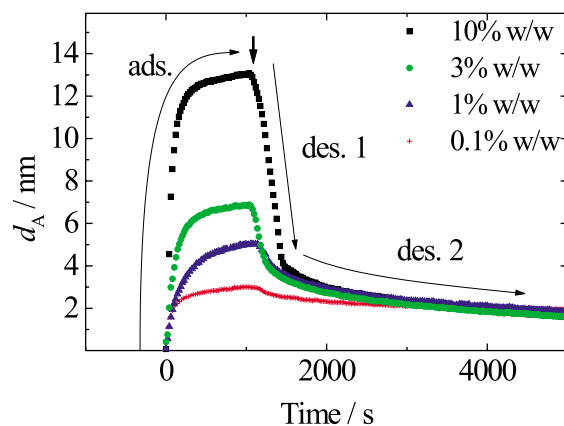


FIG. 1. (Color online) Plots of mucin film thickness d_A against time during adsorption from solutions of three different concentrations (from bottom to top, 0.1%, 1%, 3%, and 10% w/w) (respectively, red, blue, green, and black symbols) followed by (starting at the short vertical arrow) desorption during laminar flow of ultrapure water. The arrows marked “ads.,” “des.1,” and “des.2” indicate the different phases of the overall process described in the text.

$$\Delta d_F = \frac{n_o^2 - n_C^2}{n_F^2 - n_C^2} \left[\frac{(N/n_C)^2 + (N/\tilde{n})^2 - 1}{(N/n_C)^2 + (N/n_F)^2 - 1} \right]^\rho d_A \quad (3)$$

and

$$\tilde{n}^2 = n_o^2(1 - n_C^2/n_o^2)/(1 - n_C^2/n_e^2), \quad (4)$$

with $\rho = 0$ and 1 for the TE and TM modes, respectively, were then solved for $m = 0$ together with Eq. (1) to yield n_o , n_e , and d_A . The value of the cover refractive index n_C was taken to be 1.331 263 throughout, corresponding to pure water at 25.0 °C.

Figure 1 shows the evolution of d_A thus calculated from the data. Noteworthy is the fact that at long desorption times all the curves converge, yet the peak (plateau) adsorbed amounts increase with increasing bulk concentration up to the highest value that could be measured.²⁵ From these data we infer that the mucin film consists of two qualitatively different types of adsorbed molecule: (1) highly spread, presumably in an extended conformation making many contacts with the adsorbent,²⁶ and (2) random coil, with a conformation close to that of the bulk solution, these molecules being merely somewhat entangled with the highly spread ones. This has the corollary that the highly spread molecules, which have necessarily a greater contact area with the surface, desorb slowly (with stretched exponential kinetics as described in Ref. 27), and the entangled ones desorb rather rapidly. The rapid and slow desorption processes are clearly distinguished from one another (indicated by “des.1” and “des.2” on Fig. 1). Figure 2 plots the corresponding thicknesses associated with the two molecular states against bulk concentration during adsorption. The thickness of 4 nm²⁸ for the highly spread molecules corresponds to that independently inferred for a glycosylated polypeptide chain with an extended, denatured configuration²⁹ (it is the irreducible thickness associated with the oligosaccharide side chains). In its native conformation, mucin resembles a dumbbell, the two knobs at the extremities (joined by the oligosaccharide-decorated peptide backbone, which is itself 40–50 nm long)

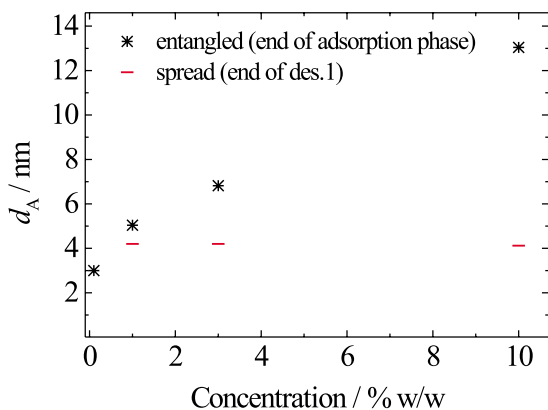


FIG. 2. (Color online) Plots of the thicknesses associated with the highly spread molecules [– (red online), associated with des.2 in Fig. 1] and the entangled molecules (*, associated with des.1) vs bulk concentration during adsorption, derived from the kinetic data shown in Fig. 1.

being polypeptide globules about 20 nm in diameter.²⁹ The thickness associated with the native, entangled molecules (crosses on Fig. 2) lies within this value.

We now turn to the anisotropy. The ordinary and extraordinary refractive indices of the adsorbed mucin film were calculated using the mode equations (2). These are plotted in Fig. 3 as their difference (the birefringence, $n_o - n_e$) against the adsorbed mass M , calculated according to³⁰

$$M = d_A \langle (n_A) - n_c \rangle / (dn/dc), \quad (5)$$

where dn/dc is the refractive index increment, determined as $0.1375 \text{ cm}^3/\text{g}$ at a wavelength of 633 nm for mucin in water at $25.0 \text{ }^\circ\text{C}$.³¹ These plots show dramatic hysteresis.

Several novel and important features are indeed apparent from these results. First, there is the significant anisotropy of the adsorbed glycoprotein films: they are birefringent even at rather low surface coverages. Second, and most prominently, there is highly significant adsorption-desorption hysteresis of birefringence, which in itself confirms the existence of multiple glycoprotein conformations. The higher the bulk glycoprotein concentration, the more prominent the hysteresis. It

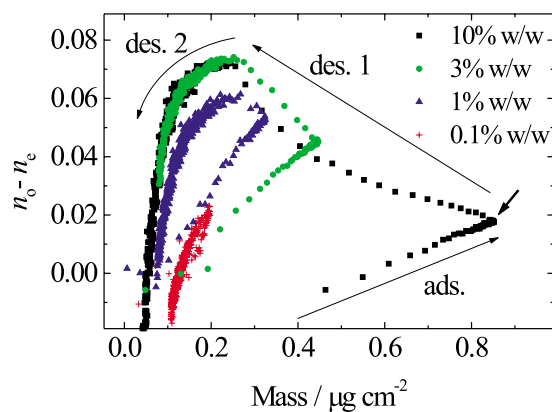


FIG. 3. (Color online) Plots of the birefringence ($n_o - n_e$) vs adsorbed mass (M) for mucin adsorbed from bulk concentrations of (lower right moving toward upper left for the adsorption phase) 10% (■), 3% (●), 1% (▲) and 0.1% (+) w/w (respectively, black, green, blue and red symbols). The cusplike feature of the extreme right of each curve (marked with the short thick arrow for the 10% data) corresponds to the point at which mucin flow was replaced by ultrapure water, i.e., when desorption commenced.

is also apparent that if only a very small amount of adsorption is allowed to take place, by arresting the flow of glycoprotein and replacing it by a flow of ultrapure water well before the layer is saturated (as shown for a mucin concentration of 0.1%), no hysteresis is observed. Furthermore, it is highly revealing that the birefringence very significantly increases during the *desorption* process, most prominently during the desorption following adsorption from the highest bulk glycoprotein concentration, before declining back to zero, or even becoming slightly negative (note that the uncertainties become large at low surface coverages), just before the mucin molecules are finally entirely removed from the adsorbent surface.

This behavior is qualitatively different from that previously observed with structurally simpler proteins. Our interpretation of these curves is as follows. The mucin molecules that first arrive at the initially unoccupied solid/liquid interface independently make multiple weak bonds with the surface (hence the molecule as a whole is quite strongly bound) and adopt a spread (extended) conformation,²⁶ which we denote as adsorbed type \mathcal{S} . We propose that this mode gives rise to the uniaxial anisotropy (note that $n_o > n_e$, conventionally called negative birefringence, indicates layering of the molecules parallel to the interface³²). Molecules arriving later under locally crowded conditions (i.e., at patches of the surface already at least partly occupied by spread molecules) do not have space to spread and are thus relatively weakly bound to the surface by a small patch (and possibly also weakly entangled with proteins in adsorbed mode \mathcal{S}): we denote them as adsorbed type \mathcal{U} (unspread), presumed to be isotropic. Molecular spreading is a relatively slow process (cf. Ref. 4), hence the lower the bulk mucin concentration (and hence the longer the intervals between consecutively arriving molecules), the greater the difference between the two modes of adsorption, and hence the faster the anisotropy grows with surface coverage (Fig. 3). As the bulk concentration increases, however, not only do molecules arrive at the surface in each other's vicinity with ever shorter intervals, and therefore occupy space without finding time to spread and develop anisotropy, but they also will increasingly be somewhat entangled with their congeners in solution (the semientangled regime) and may be only partially disentangled when they arrive at the surface. However, there is no evidence that entanglement with molecules of adsorbed type \mathcal{U} results in the formation of an additional layer.

Sudden dilution of the system (such as occurs upon making ultrapure water flow through the microcuvette) initially removes the weakly entangled molecules only.³³ In the case of adsorption from the highest bulk concentration, these molecules make up the majority of the adsorbed film (type \mathcal{U}). The removal of some of them creates space at the surface for those initially remaining, which then spread into an extended conformation (cf. Ref. 7), thus becoming transformed into type \mathcal{S} and increasing the birefringence. The hysteresis loops show maximum birefringence (Fig. 3) precisely at the point when this process is concluded. As the spread molecules are themselves then slowly removed, the birefringence also slowly drops toward zero (the birefringence of a very sparse film is, in fact, indeterminate) with the stretched exponential

kinetics previously observed.²⁷ The higher the bulk mucin concentration (and hence the greater the population of type U at the surface, able to convert to type S), the greater is the growth of birefringence during desorption. It is apparent from Fig. 1 that desorption from the layers assembled from the two highest bulk mucin concentrations is slightly slower for the first few tens of seconds than later, possibly suggesting the existence of a third molecular state, possibly one that is slightly more entangled with other adsorbed molecules. Note that the mucin-water system is very favorable for observing these effects, not least because both adsorption and desorption occur on accessible time scales.

Thin films assembled from objects of order of 10 nm in size can and often have been modeled as homogeneous, isotropic films characterized by a geometric thickness and a single refractive index.²⁰ Such a model fails to describe thin films assembled from the glycoprotein mucin in solution, however. Modeling the films as uniaxially anisotropic reveals two principal molecular states whose interplay governs the structure of the film formed under a given set of conditions. This kind of structure and the mechanism by which it is formed—initial adsorption from a low bulk concentration in an extended conformation, but predominantly in a compact conformation from a high bulk concentration, converting to the extended conformation when some of the molecules are allowed to desorb—could be, we propose, a general feature of the self-assembly of large glycoproteins.

Inter alia, we expect that this knowledge will be highly relevant for understanding the extraordinary effectiveness of mucin as a boundary lubricant. Although mucin is an amazingly ubiquitous natural lubricant, it by no means follows that it is adapted to lubricating artificial implants that share a common environment with the remaining natural components of a joint that has undergone repair. It is therefore very important to understand the principles of mucin lubrication and the molecular level, not least in order to be able to design better biomimetic surfaces for artificial implants, in order to make them fully biocompatible. The approach that we have developed in this paper is generally valid for understanding the richness of behavior that might be expected for a great variety of complex glycoproteins, which are just beginning to be isolated from living systems and investigated in molecular detail.

¹L. A. Blumenfeld, *Problems of Biological Physics* (Springer, Heidelberg, 1981).

²J. J. Ramsden, in *Complexity and Security*, edited by J. J. Ramsden and P.

- J. Kervalishvili (IOS, Amsterdam, 2008), pp. 93–102.
- ³J. Talbot, *Adsorption* **2**, 89 (1996).
- ⁴J. J. Ramsden, *Phys. Rev. Lett.* **71**, 295 (1993).
- ⁵R. Kurrat, J. J. Ramsden, and J. E. Prenosil, *J. Chem. Soc., Faraday Trans.* **90**, 587 (1994).
- ⁶R. Kurrat, J. E. Prenosil, and J. J. Ramsden, *J. Colloid Interface Sci.* **185**, 1 (1997).
- ⁷P. R. Van Tassel, L. Guemouri, J. J. Ramsden, G. Tarjus, P. Viot, and J. Talbot, *J. Colloid Interface Sci.* **207**, 317 (1998).
- ⁸L. Guemouri, J. Ogier, Z. Zekhnini, and J. J. Ramsden, *J. Chem. Phys.* **113**, 8183 (2000).
- ⁹Ph. Roussel and Ph. Delmotte, *Curr. Org. Chem.* **8**, 413 (2004).
- ¹⁰R. Bansil and B. S. Turner, *Curr. Opin. Colloid Interface Sci.* **11**, 164 (2006).
- ¹¹K. Tiefenthaler and W. Lukosz, *J. Opt. Soc. Am. B* **6**, 209 (1989).
- ¹²J. J. Ramsden, *J. Stat. Phys.* **73**, 853 (1993).
- ¹³J. J. Ramsden, in *Proteins at Solid-Liquid Interfaces*, edited by Ph. De-jardin (Springer, Heidelberg, 2006), pp. 23–49.
- ¹⁴J. J. Ramsden, *Biopolymers* **33**, 475 (1993).
- ¹⁵R. Horvath and J. J. Ramsden, *Langmuir* **23**, 9330 (2007).
- ¹⁶J. R. Lu, in *Surfaces and Interfaces for Biomaterials*, edited by P. Vad-gama (Woodhead, Abington, 2005), pp. 299–321.
- ¹⁷C. Viney, A. Huber, and P. Verdugo, *Macromolecules* **26**, 852 (1993).
- ¹⁸G. E. Yakubov, A. Papagiannopoulos, E. Rat, and T. A. Waigh, *Biomacromolecules* **8**, 3791 (2007).
- ¹⁹G. E. Yakubov, H.-J. Butt, and O. I. Vinogradova, *J. Phys. Chem. B* **104**, 3407 (2000).
- ²⁰E. K. Mann, L. Heinrich, and P. Schaaf, *Langmuir* **13**, 4906 (1997).
- ²¹This equation is derived by noting that it is the dielectric constants (the squares of the refractive indices) that should be averaged. Furthermore, in a uniaxial crystal two of the three axes of the index ellipsoid are equivalent.
- ²²This is a reasonable estimate, in accord with various measurements, made with more or less reliable assumptions, scattered in the literature. It is also in accord with rather reliable measurements of the refractive index increments of protein solutions and estimates of the mass density of adsorbed protein layers (approximately 0.6 g/cm³).
- ²³W. Lukosz, *Biosens. Bioelectron.* **12**, 175 (1997).
- ²⁴R. Horvath, G. Fricsovszky, and E. Papp, *Biosens. Bioelectron.* **18**, 415 (2003).
- ²⁵Beyond a concentration of about 10% (w/w), the glycoprotein solutions become extremely viscous and difficult to manipulate experimentally.
- ²⁶A. Fernández and J. J. Ramsden, *J. Biol. Phys. Chem.* **1**, 81 (2001).
- ²⁷J. McColl, G. E. Yakubov, and J. J. Ramsden, *Langmuir* **23**, 7096 (2007).
- ²⁸Compare scratch tests made with an atomic force microscope, which yielded a thickness of about 4 nm.
- ²⁹G. E. Yakubov, A. Papagiannopoulos, E. Rat, R. L. Easton, and T. A. Waigh, *Biomacromolecules* **8**, 3467 (2007).
- ³⁰V. Ball and J. J. Ramsden, *Biopolymers* **46**, 489 (1998).
- ³¹For all practical purposes, i.e., within the experimental uncertainty of the measurement, the M thus calculated is the same as that obtained by substituting $\langle n_A \rangle$ and d_A in Eq. (5) by the unrealistic refractive index and thickness calculated from the homogeneous and isotropic analysis (cf. Ref. 15).
- ³²O. Wiener, *Abh. math.-phys. Kl. königl. sächs. Ges.-Wiss.* **32**, 503 (1912).
- ³³Atomic force microscopy carried out at this point reveals holes in the protein layer.